Atmospheric
Chemistry
and Physics
Discussions

Inconsistent decadal variations between surface and free tropospheric nitrogen oxides over United States

Zhe Jiang[1], Helen Worden[1], John R. Worden[2], Daven K. Henze[3], Dylan B. A. Jones[4], Avelino F. Arellano[5], Emily V. Fischer[6], Liye Zhu[6], Kazuyuki Miyazaki [2,7], K. Folkert Boersma[8,9], Vivienne H. Payne[2],

[1]National Center for Atmospheric Research, Boulder, CO, USA
[2]Jet Propulsion Laboratory, California Institute of Technology, Pasadena, CA, USA
[3]Department of Mechanical Engineering, University of Colorado, Boulder, CO, USA
[4]Department of Physics, University of Toronto, Toronto, ON, Canada
[5]Department of Hydrology and Atmospheric Sciences, University of Arizona, Tucson, AZ, USA
[6]Department of Atmospheric Science, Colorado State University, Fort Collins, CO, USA
[7]Japan Agency for Marine-Earth Science and Technology, Yokohama, Japan
[8]Wageningen University, Meteorological and Air Quality department, Wageningen, the Netherlands
[9]Royal Netherlands Meteorological Institute, De Bilt, The Netherlands

Atmospheric
Chemistry
and Physics
Discussions

34   **Abstract**

35   Decreases in surface emissions of nitrogen oxides ($NO_x = NO + NO_2$) in North America have led

36   to substantial improvements in air-quality over the last several decades. Here we show that satellite

37   observations of tropospheric nitrogen dioxide (NO_2) columns over the contiguous United States

38   (US) do not decrease after about 2009, while surface NO_2 concentrations continue to decline

39   through to the present. This divergence, if it continues, could have a substantial impact on surface

40   air quality due to mixing of free-tropospheric air into the boundary layer. Our results show only

41   limited contributions from local effects such as fossil fuel emissions, lightning, or instrument

42   artifacts, but we do find a possible relationship of NO_2 changes to decadal climate variability. Our

43   analysis demonstrates that the intensity of transpacific transport is stronger in El Niño years and

44   weaker in La Niña years, and consequently, that decadal-scale climate variability impacts the

45   contribution of Asian emissions on North American atmospheric composition. Because of the short

46   lifetime, it is usually believed that the direct contribution of long-range transport to tropospheric

47   NO_x distribution is limited. If our hypothesis about transported Asian emissions is correct, then

48   this observed divergence between satellite and surface NO_x could indicate mechanisms that allow

49   for either NO_x or its reservoir species to have a larger than expected effect on North American

50   tropospheric composition. These results therefore suggest more aircraft and satellite studies to

51   determine the possible missing processes in our understanding of the long-range transport of

52   tropospheric NO_x.

53

54   **1. Introduction**

55   Nitrogen oxides play a complex role in tropospheric chemistry and have a strong influence

56   on air quality as precursors in the formation of ozone (O_3) and secondary aerosols. Tropospheric

Atmospheric
Chemistry
and Physics
Discussions

Open Access

57   NO_x is produced through anthropogenic combustion, biomass burning, soil (Jaegle et al., 2005),

58   and lightning emissions (Schumann and Huntrieser, 2007), and is mainly removed by the

59   formation of nitric acid (HNO_3). Most NO_x is emitted as nitric oxide (NO), however, it is most

60   appropriate to consider the budget of the NO_x as a whole, because of the rapid cycling between

61   NO and NO_2 (~ 1 min). Tropospheric NO_x has short lifetime, a few hours except in extratropical

62   winter when it increases to 1-2 days (Martin et al. 2003).

63   Because of the short lifetime, state of the art chemistry/climate models suggest that the

64   direct contribution of long-range transport to tropospheric NO_x distribution is limited (e.g. Zhang

65   et al. 2008). However, NO_x can also be transported far away from the sources via the formation of

66   long-lived reservoir species, such as peroxyacetyl nitrate (PAN, e.g., Fischer et al., 2014; Jiang et

67   al. 2016a). Models have large uncertainties in PAN abundance (Fischer et al., 2014) and there are

68   also potentially other missing processes in the chemical transport models used to diagnose NO_x

69   lifetime and transport. For example, a recent discovery about the rapid cycling of reactive nitrogen

70   in the marine boundary layer (Ye et al. 2016) demonstrates processes that are not represented in

71   modeled NO_x transport, and that may help explain existing discrepancies in reactive nitrogen

72   partitioning between models and observations.

73   Due to its critical influence in the troposphere, there are multiple space-based

74   measurements for tropospheric NO_2 that are available from satellites that were launched in the past

75   two decades. These instruments typically measure backscattered solar radiation from which the

76   vertically integrated column abundance of NO_2 is retrieved. The assumption of weak long-range

77   transport allows relatively simple applications of the space-based NO_2 column data to study NO_x

78   sources. For example, recent studies (e.g. Reuter et al. 2014; Itahashi et al. 2014; Duncan et al.

79   2016; Krotkov et al. 2016) assessed the trends of surface NO_x emissions by assuming a strong

Atmospheric
Chemistry
and Physics
Discussions

80   correlation between tropospheric NO_2 columns with local emissions. The tropospheric NO_2

81   column data are also widely used in inverse modeling analyses to estimate NO_x emissions by either

82   scaling the surface NO_x emissions with the corresponding ratio of observed over modeled

83   tropospheric NO_2 column (e.g. Lamsal et al. 2011; Mijling et al. 2012; Gu et al. 2014) or through

84   data assimilation techniques with short localization length scales (e.g. Miyazaki et al. 2017).

85   Since 1990, US regulations have required significant NO_x emission reductions over many

86   regions (US Environmental Protection Agency, 2010). The trend of decreasing local US NO_x

87   emissions has been confirmed by several studies (e.g. Lamsal et al. 2015; Tong et al. 2015; Kharol

88   et al. 2015; Duncan et al. 2016; Krotkov et al. 2016). In contrast to the decreasing local NO_x

89   emissions, recent studies (e.g. Cooper et al. 2010; Verstraeten et al. 2015) have indicated an

90   increase in free tropospheric O_3 over western North America over the past decade. The discrepancy

91   between variations of local NO_x emissions and free tropospheric O_3 suggests possible influences

92   from non-local sources, and consequently, provides motivation to re-evaluate the contribution of

93   long-range transport to the free tropospheric NO_x distribution.

94   In this work, we investigate the variation of US tropospheric NO_2 in the past decade to

95   assess the contribution of non-local sources. We will particularly explore the possible answers for

96   the following questions: why there is good agreement between tropospheric NO_2 column and

97   surface measurements over the period of 2005-2008? What is the reason for the appearance of the

98   large and growing divergence at around 2009? What is the impact of the decreasing Chinese NO_x

99   emissions since 2013 (Liu et al. 2016) on North America? To evaluate these critical questions,

100   multiple data sets and model are used in this work, including remotely sensed NO_2 column

101   measurements from Ozone Monitoring Instrument (OMI, NASA and DOMINO products), in-situ

102   surface NO_2 measurements from the Environmental Protection Agency (EPA) Air Quality System

103   (AQS) network and the Environment Canada National Air Pollution Surveillance Program (NAPS)

104   network, flash rate density data from Lightning Imaging Sensor (LIS), and the GEOS-Chem

105   chemical transport model.

106   This paper is organized as follows: in Section 2 we describe the observations and model

107   used in this work. In Section 3 we demonstrate the divergence between the OMI NO_2 column

108   retrievals and surface measurements over the period of 2005-2015 and focus on the evaluation of

109   contributions from various hypotheses that could explain the divergence. Our conclusions follow

110   in Section 4.

111   **2. Observations and Models**

112   **2.1 Tropospheric NO_2 column from OMI**

113   The OMI instrument was launched on NASA's Aura spacecraft. The sensor has a spatial

114   resolution of 13 km x 24 km. OMI provides daily global coverage with measurements of both

115   direct and atmosphere-backscattered sunlight in the ultraviolet-visible range from 270 to 500 nm;

116   the spectral range 405-465 nm is used to retrieve tropospheric NO_2 columns. Two versions of the

117   OMI retrievals (level 2) are used in this work: the NASA (version 3, Krotkov and Veefkind 2006;

118   Bucsela et al. 2013) and DOMINO (version 2, Boersma et al. 2011) retrievals. There are significant

119   differences in the retrieval algorithms of the two products. For example, the a priori NO_2 profiles

120   of the NASA product is based on data from the Global Modeling Initiative (GMI) model with

121   yearly varying emissions, whereas the a priori NO_2 profiles of the DOMINO product is from the

122   Tracer Model 4 (TM4) without interannual variations in emissions. In addition, for the NASA

123   product, the stratospheric contribution to the tropospheric column is estimated from the GMI

124   model simulation. In contrast, for the DOMINO product, the stratospheric contribution is based on

125   the assimilation of OMI data into the TM4 model.

Atmospheric
Chemistry
and Physics
Discussions

126   Starting in 2007, anomalies were found in OMI data and diagnosed as attenuated measured

127   radiances in certain cross-track positions. This instrument degradation has been referred to as the

128   "row anomaly". In order to ensure the quality and stability of the data, the following filters are

129   applied in our analysis for both OMI products (NASA and DOMINO):

130   1) Tropospheric Column Flag = 0

131   2) Surface Albedo < 0.3

132   3) Cloud Radiance Fraction < 0.5

133   4) No edge data (rows 1-5, 56-60)

134   5) No row anomaly data (rows 27-55 for the whole period 2005-2015)

135   After the application of the filters, the number of measurements over the US is about 185,000 per

136   month in 2010. Thus, we expect the uncertainties in the monthly/annual mean NO_2 columns due

137   to random errors are small. The discrepancy between the two OMI products (see Figures 1a-b) is

138   mainly caused by the two different retrieval algorithms.

139   **2.2 AQS and NAPS surface in-situ NO_2 concentration**

140   We use daily-averaged in-situ surface NO_2 measurements from the EPA AQS network,

141   and the Environment Canada NAPS network. The AQS/NAPS networks collect ambient air

142   pollution data from monitoring stations located in urban, suburban, and rural areas. In the analysis

143   here, the daily data are averaged to obtain monthly mean concentration at each station.

144   **2.3 Flash rate density from Lightning Imaging Sensor (LIS)**

145   LIS is a component of the NASA Tropical Rain Measuring Mission (TRMM). It measures

146   total optical pulses from cloud-to-ground and intracloud lightning flashes during both day and

147   night with global coverage (42.5°S-42.5°N) in the period 1995-2014. Monthly flash rate density

148   (flash/km2) with 2.5°x2.5° resolution is used in this work (Cecil et al. 2006).

149   **2.4 NOAA Niño 3.4 index**

150   The Niño 3.4 index comprises sea surface temperature averaged across the region (5°S–

151   5°N, 170°W–120°W), and their monthly anomalies relative to the 1982–2015 means to constitute

152   the indices. Years with positive values (>0.5) are considered as El Niño, whereas years with

153   negative values (< -0.5) are considered as La Niña.

154   **2.5 Passive tracer simulation using GEOS-Chem model**

155   The GEOS-Chem global chemical transport model (CTM) [www.geos-chem.org] is driven

156   by assimilated meteorological fields (MERRA) from the NASA Goddard Earth Observing System

157   at the Global Modeling and data Assimilation Office. We use version v9-01-03 of GEOS-Chem at

158   a horizontal resolution of 4°x5°. Bertram et al. (2013) indicated the dominant role of long-lived

159   reservoir species in the transpacific transport of reactive nitrogen using aircraft measurements from

160   the INTEX-B campaign. Although the lifetime of tropospheric NO_x is short, the lifetime of long-

161   lived reservoir species is much longer, for example, the lifetime of free tropospheric PAN is about

162   1 month. In order to assess the effects of physical transport processes on the long-range transport

163   of reactive nitrogen, we performed a "passive" tracer simulation, with a constant and uniform

164   timescale for loss of 15 days (i.e. 360 hours) over the period of 2005-2015 following the approach

165   of Jiang et al. (2016b). The global a priori surface NO_x emissions (anthropogenic, biomass burning

166   and soil emissions) are fixed at 2005 level. For each time step (one hour), the tropospheric NO_2 is

167   calculated by: $NO_2^t = NO_2^{t-1} e^{-1/360}$. The lightning NO_x emissions are not included in the

168   simulation. The 15-day lifetime was selected to provide an approximation for the variation of free

169   tropospheric NO_x via the formation and transport of long-lived reservoir species, due to changes

170   in meteorology. Although actual lifetimes of long-lived reservoir species will vary, we found that

171   15-days was a reasonable compromise to understand the influence of decadal-scale variability on

172   long-range transport patterns.

3. Results and Discussion

174   Figures 1a-b show the variations of mean tropospheric NO_2 columns from OMI (NASA

175   and DOMINO products) over the US and east China, respectively. Although there is a significant

176   bias in the magnitude of tropospheric NO_2 column between two OMI products, indicating the

177   influence of different retrieval algorithms, this bias should not affect the trend analysis, as

178   demonstrated by the consistent interannual variations between the two data products. Figure 1c

179   shows percent changes, relative to 2009, of the annual mean tropospheric NO_2 columns over the

180   US, and of the total US NO_x emissions (anthropogenic + biomass burning) from the US EPA

181   (https://www.epa.gov/air-emissions-inventories/air-pollutant-emissions-trends-data). There is

182   good agreement between the changes in the OMI retrievals and the emissions estimates in the

183   2005-2009 period: the annual slope of the EPA's estimates is -6.4%±0.03% (slope of linear

184   regression ± uncertainty of slope), and the annual slopes of the two sets of OMI retrievals are -

185   6.8%±1.1% (NASA) and -8.0%±0.8% (DOMINO). Conversely, we find a large, growing

186   separation in the 2009-2015 period: the annual slope of the EPA's estimates is -4.6%±0.03%,

187   whereas the annual slopes of OMI retrievals are -0.5%±0.6% (NASA) and 1.6%±1.1%

188   (DOMINO). Figures 1d-e show the percent changes in the seasonal mean tropospheric NO_2

189   columns from OMI retrievals, and in the EPA's estimates (annual mean). The divergence between

190   the seasonal NO_2 columns and the emissions is similar to that shown in Figure 1c, suggesting there

191   is no obvious seasonal dependence.

192   Our intention here is to understand the possible reasons for the divergence between

193   observed changes in NO_2 vs. changes expected from NO_x emissions. Figure 2 depicts the potential

194   hypotheses that could explain the divergence:

Atmospheric
Chemistry
and Physics
Discussions

195   • Hypothesis 1 (H1): Increasing local NO_x emissions missing from the EPA inventories

196   • Hypothesis 2 (H2): Time dependent OMI retrieval errors

197   • Hypothesis 3 (H3): Non-local sources

198   **3.1 Increasing local NO_x emissions (H1)**

199   Figure 3a shows the differences of mean surface NO_2 concentrations, as measured by the

200   AQS and NAPS network, from 2009-2010 to 2014-2015. These time periods were chosen to

201   determine changes in surface NO_2 concentrations over the period of 2009-2015 with sufficient

202   stattistics. Figure 3b shows the same variations averaged with 4°x5° resolution (i.e., at the GEOS-

203   Chem grid points). The surface stations demonstrate dramatic decreases of surface NO_2

204   concentrations in the period of 2009-2015. The consistent decreasing trends in the surface NO_2

205   concentrations and the EPA's emission estimates during the period of 2009-2015 suggests that the

206   divergence between the OMI retrievals and the EPA's emission estimates is not caused by US

207   local emissions. We note that our analysis based on surface in-situ measurements may not provide

208   sufficient representation for emissions from oil and gas exploration and production. However,

209   though potentially important locally, these activities only contribute about 5% to total US NO_x

210   emissions based on EPA's estimates. Therefore, we do not expect significant contributions to the

211   overall changes in tropospheric NO_2 from these sources.

212   Similarly, we expect limited contributions from other sources which are not included in

213   EPA's inventory. The contribution from aircraft NO_x is only about 3% of total US NO_x emissions

214   (Skowron et al. 2014). Soil NO_x emissions account for up to 40% of the tropospheric NO_2 columns

215   in summer over US rural areas (Hudman et al. 2010), but only contribute a few percent of the US

216   annual mean tropospheric NO_2 column. Similarly, NO_x production by lightning is stronger in

217   summer, with an estimated annual contribution of 15% to the total emissions. Because the

218   discrepancies between the OMI retrieveals and the EPA's emission estimates lack a clear seasonal

219   dependence (see Figures 1d-e), we expect negligible contributions from soil and lightning NO_x

220   emissions to the enhanced tropospheric NO_2 in the period of 2009-2015. Furthermore, Figure 4

221   indicates that the flash rate density over North America from LIS is uncorrelated with the observed

222   NO_2 variation.

223   3.2 Time dependent OMI retrieval errors (H2)

224   The quality of the OMI retrievals has been evaluated with surface in-situ measurements.

225   Lamsal et al. (2015) reported that the correlation between OMI NO_2 tropospheric columns (NASA)

226   and the AQS surface in-situ NO_2 measurements was 0.68 for the period 2005-2010. Hoek et al.

227   (2015) indicated that the correlation between the OMI NO_2 tropospheric columns (DOMINO) and

228   surface in-situ measurements in the Netherlands was 0.74 at 2007. The stability of our analysis

229   based on OMI retrievals (NASA and DOMINO) is ensured by the strict quality filters; these ensure

230   that changes in OMI sampling due to detector problems (e.g. row anomaly) do not affect our

231   conclusions.

232   Figure 5 shows the annual slopes of tropospheric NO_2 columns from OMI (NASA and

233   DOMINO) over the period of 2005-2015. Both OMI products (NASA and DOMINO), with

234   various a priori models (GMI and TM4) and algorithms, show consistent variations over the

235   northern Pacific Ocean and the western US: insignificant changes in the period 2005-2008 (Figure

236   5a-b), positive changes in the period 2009-2012 (Figure 5c-d) and insignificant changes in the

237   period 2013-2015 (Figure 5e-f). Using the Berkeley High-Resolution (BEHR) NO_2 product for

238   OMI, Russell et al. (2012) obtained similar positive change over the western US with the Weather

239   Research Forecasting Chemistry model (WRF-Chem) as an a priori model in the period 2005-

240   2011. The consistency among the various data products suggests that the variations in the retrieved

241   OMI NO_2 over the period of 2005-2015 are not caused by systematic biases.

242   While our adherence to published data quality filters should ensure the observed OMI

243   based NO_2 values are robust, we note as a caveat that we cannot unequivocally confirm these

244   changes with independent data due to a lack of either total column or free-tropospheric NO_2

245   measurements over the observed region. For example, Mt. Bachelor Observatory (MBO) station

246   has free troposheric NO_2 observations in the period of 2005-2009 and the CARIBIC aircraft

247   measurements only provide free tropospheric NO_2 observations over the US since 2014. Using

248   remotely sensed NO_2 measurements from the Global Ozone Monitoring Experiment-2 (GOME-

249   2), Miyazaki et al. (2017) found a slight increase of tropospheric NO_2 columns over the US in the

250   period of 2009-2012, consistent with our result. However, a significant sudden decrease of

251   retrieved tropospheric NO_2 columns from GOME-2 has been observed since July 2013, associated

252   with the change in the measurement mode (http://projects.knmi.nl/atcom/ news.php?id=44).

253   **3.3 Non-local sources (H3)**

254   We have demonstrated that hypotheses H1 and H2 are not likely the dominant factors,

255   which leaves hypothesis H3 (non-local sources) as possible important contributors. Figures 5g-h

256   show the annual slope of tropospheric NO_2 columns (percent base) from OMI (NASA and

257   DOMINO) over the period of 2009-2015. Our analysis demonstrates a significant positive change

258   over the northern Pacific Ocean during this time period, and an insignificant but positive change

259   over the western US, suggesting possible contributions from transpacific transport to tropospheric

260   NO_2 over the western US. Over the period of 2005-2008, the lack of change in tropospheric NO_2

261   columns over the northern Pacific Ocean (Figure 5a-b) indicates the dominant role of local sources

262   to the decrease of US tropospheric NO_2 in this period. Conversely, the increase in tropospheric

263   NO_2 columns over northern Pacific Ocean over the period of 2009-2012 (Figure 5c-d) is consistent

Atmospheric
Chemistry
and Physics
Discussions

264   with the appearance of a discrepancy between the OMI retrievals and EPA's emission estimates

265   (Figure 1c). Accompanying with the observed decrease of Chinese NO_2 emissions (Figure 1b), no

266   significant change is observed over the northern Pacific Ocean over the period of 2013-2015

267   (Figure 5e-f).

268   Decadal climate variability has non-negligible influences on tropospheric compositions by

269   affecting the physical and chemical processes. For example, Lin et al. (2014) indicated that

270   transpacific transport of O_3 is modulated by decadal variability of El Niño–Southern Oscillation

271   (ENSO). El Niño is defined as the appearance of anomalously warm water off northern Peru and

272   Ecuador in December. The atmospheric component tied to El Niño is called the Southern

273   Oscillation (Trenberth 1997). To the best of our understanding, ENSO is the dominant climate

274   phenomenon linked to extreme weather conditions globally (Cai et al. 2015), and it also exerts a

275   major influence on the interannual variability of O_3 in the troposphere (Doherty et al., 2006).

276   Following Jiang et al. (2016b), we conducted an analysis using an idealized passive tracer to assess

277   the possible influences of transport patterns. We performed a GEOS-Chem model simulation for

278   tropospheric NO_2 over the period of 2005-2015 with an NO_2-like tracer with a constant 15-day

279   lifetime and fixed (2005 level) surface NO_x emissions. The passive tracer simulation with constant

280   lifetime avoids the possible influences from uncertainties in the modeled nonlinear NO_x chemistry,

281   particularly, the conversion between NO_x and its longer-lived reservoir species.

282   Figures 6a-c show that even with emissions held constant, interannual variations in

283   transport produce differences in NO_2 (or the passive tracer) columns over the eastern Pacific.

284   Based on the passive tracer simulation, transpacific transport decreased over the period of 2005-

285   2008 (Figure 5a). During this four-year period, declining transport efficiency appears to have offset

286   the increase of Asian emissions, resulting in insignificant changes of tropospheric NO_2 columns

287 over the northern Pacific Ocean (Figures 5a-b), and consequently, good agreement between the

288 OMI retrievals and the EPA's emission estimates (Figure 1c). The efficiency of transpacific

289 transport is more stable over the period of 2009-2012 (Figure 6b), which allows stronger

290 transpacific transport of rising Asian emissions. It leads to positive changes of tropospheric NO_2

291 columns over the northern Pacific Ocean (Figure 5c-d), and consequent growing discrepancy

292 between the OMI retrievals and the EPA's emission estimates (Figure 1c). Increasing efficiency

293 in transpacific transport over the period of 2013-2015 (Figure 6c) counteracts the decrease of

294 Chinese NO_2 (Figure 1b), again resulting in no change in the tropospheric NO_2 column over

295 northern Pacific Ocean (Figure 5e-f) and relatively flat changes in US tropospheric NO_2 column.

296 Figure 6d shows the comparison between regional mean of passive tracer columns over the

297 northern Pacific Ocean with the NOAA Niño 3.4 index. There is strong correlation between

298 transpacific transport and ENSO: the transpacific transport is stronger in El Niño years and weaker

299 in La Niña years, demonstrating strong influence of decadal climate variability on the transpacific

300 transport.

301 Brown-Steiner et al. (2011) showed that Asian O_3 is transported across Pacific Ocean

302 primarily in the lower/middle troposphere in winter and spring, and primarily in the middle/upper

303 troposphere in summer and fall, but that differences in tropospheric column remain small for

304 different seasons. Figure 7 shows the seasonal mean tropospheric columns for the NO_2-like tracer

305 between 2005-2015. Our analysis indicates the transpacific transport, with constant 15-day lifetime,

306 is strongest in summer and spring. However, the lifetime of PAN approximately doubles for every

307 4°C decrease in temperature. Consequently, due to the temperature effect associated with the

308 change in transport pathways from the lower troposphere (in spring) to the upper troposphere (in

309 fall), transport in fall, relative to that in spring, should be greater than that shown in Figure 7c.

Atmospheric
Chemistry
and Physics
Discussions

310   Similarly, the actual transpacific transport of NO_2 in winter, relative to that in spring, should be

311   greater than shown in Figure 7d because of the temperature differences between winter and spring.

312   Thus, in agreement with Brown-Steiner et al. (2011), our analysis would suggest weak seasonality

313   of transpacific transport of reactive nitrogen, consistent with the observed changes in OMI NO_2

314   over the US (Figures 1d-e). It should be noticed that our conclusion about weak seasonality of

315   transpacific transport is different from previous studies (e.g. Liang et al. 2004) based on carbon

316   monoxide (CO) simulations. The discrepancy in the seasonality is associated with the strong

317   springtime biomass burning CO emissions in southeast and boreal Asia, whereas the contribution

318   of biomass burning to tropospheric NO_x is relatively small.

319   **4. Conclusions**

320   In this work, we investigated the variation of US tropospheric NO_2 in the past decade, to

321   evaluate the contribution of non-local sources to the tropospheric NO_x budget. We demonstrated

322   significant divergence between the time variation in tropospheric NO_2 columns from the OMI

323   retrievals and the EPA's NO_x emission estimates. Our analysis suggests limited contributions from

324   local effects such as fossil fuel emissions, lightning, or instrument artifacts, and indicates possible

325   important contributions from long-range transport of Asian emissions that are modulated by ENSO.

326   Passive tracer simulation with fixed emissions demonstrates that the intensity of transpacific

327   transport is stronger in El Niño years and weaker in La Niña years. The unexpected important

328   contributions from long-range transport contradict assumptions of weak long-range transport for

329   NO_x, suggesting potential underestimation of transported reactive nitrogen in the state of the art

330   models.

331   In related studies, long-term free tropospheric O_3 observations over Europe demonstrated

332   a significant increase in the past three decades (e.g. Logan et al. 2012; Parrish et al. 2012), whereas

Atmospheric
Chemistry
and Physics
Discussions

333   state of the art models cannot reproduce this variation (Parrish et al. 2014). Enhanced long-range

334   transport of NO_x could potentially reconcile the large discrepancy between modeled and observed

335   free tropospheric O_3 over Europe. Because of uncertain processes in the long-range transport of

336   reactive nitrogen (Ye et al. 2016) and the dominant role of long lifetime reservoirs (Bertram et al.

337   2013), we are not able to quantify the different contributions to the observed tropospheric NO_x in

338   this study. This quantification will require comprehensive observations and modeling efforts to

339   understand the formation and transport of long lifetime reservoirs of reactive nitrogen.

340

351

352   **Reference:**

353   Bertram, T., Perring, A., Wooldridge, P., Dibb, J., Avery, M. and Cohen, R.: On the export of

354   reactive nitrogen from Asia: NOx partitioning and effects on ozone, Atmos Chem Phys, 13(9),

355   4617–4630, doi:10.5194/acp-13-4617-2013, 2013.

Atmospheric
Chemistry
and Physics
Discussions

356   Boersma, K., Eskes, H., Dirksen, R., A, R., Veefkind, J., Stammes, P., Huijnen, V., Kleipool, Q.,

357   Sneep, M., Claas, J., Leitão, J., Richter, A., Zhou, Y. and Brunner, D.: An improved

358   tropospheric NO2 column retrieval algorithm for the Ozone Monitoring Instrument,

359   Atmospheric Meas Techniques, 4(9), 1905–1928, doi:10.5194/amt-4-1905-2011, 2011.

360   Brown- Steiner, B. and Hess, P.: Asian influence on surface ozone in the United States: A

361   comparison of chemistry, seasonality, and transport mechanisms, J Geophys Res Atmospheres

362   116, D17309, doi:10.1029/2011JD015846, 2011.

363   Bucsela, E., Krotkov, N., Celarier, E., Lamsal, L., Swartz, W., Bhartia, P., Boersma, K., Veefkind,

364   J., Gleason, J. and Pickering, K.: A new stratospheric and tropospheric NO2 retrieval algorithm

365   for nadir-viewing satellite instruments: applications to OMI, Atmospheric Meas Techniques,

366   6(10), 2607–2626, doi:10.5194/amt-6-2607-2013, 2013.

367   Cai, W., Santoso, A., Wang, G., Yeh, S.-W., An, S.-I., Cobb, K., Collins, M., Guilyardi, E., Jin,

368   F.-F., Kug, J.-S., Lengaigne, M., McPhaden, M., Takahashi, K., Timmermann, A., Vecchi, G.,

369   Watanabe, M. and Wu, L.: ENSO and greenhouse warming, Nat Clim Change, 5(9), 849–859,

370   doi:10.1038/nclimate2743, 2015.

371   Cecil, D. J.: LIS/OTD 2.5 Degree Low Resolution Monthly Time Series (LRMTS). Dataset

372   available online from the NASA Global Hydrology Resource Center DAAC, Huntsville,

373   Alabama, U.S.A, 2006.

374   Cooper, O., Parrish, D., Stohl, A., Trainer, M., Nédélec, P., Thouret, V., Cammas, J., Oltmans, S.,

375   Johnson, B., Tarasick, D., Leblanc, T., McDermid, I., Jaffe, D., Gao, R., Stith, J., Ryerson, T.,

376   Aikin, K., Campos, T., Weinheimer, A. and Avery, M.: Increasing springtime ozone mixing

377   ratios in the free troposphere over western North America, Nature, 463(7279), 344–348,

378   doi:10.1038/nature08708, 2010.

Atmospheric
Chemistry
and Physics
Discussions

379   Doherty, Stevenson, Johnson, Collins and Sanderson: Tropospheric ozone and El Niño–Southern

380   Oscillation: Influence of atmospheric dynamics, biomass burning emissions, and future climate

381   change, J Geophys Res Atmospheres, 111, D19304, doi:10.1029/2005JD006849, 2006.

382   Duncan, B., Lamsal, L., Thompson, A., Yoshida, Y., Lu, Z., Streets, D., Hurwitz, M. and Pickering,

383   K.: A space-based, high-resolution view of notable changes in urban NOx pollution around the

384   world   (2005–2014),   J   Geophys   Res   Atmospheres,   121(2),   976–996,

385   doi:10.1002/2015JD024121, 2016.

386   Fischer, E., Jacob, D., Yantosca, R., Sulprizio, M., Millet, D., Mao, J., Paulot, F., Singh, H., Roiger,

387   A., Ries, L., Talbot, R. W., Dzepina, K. and Deolal, S.: Atmospheric peroxyacetyl nitrate

388   (PAN): a global budget and source attribution, Atmos Chem Phys, 14(5), 2679–2698,

389   doi:10.5194/acp-14-2679-2014, 2014.

390   Gu, D., Wang, Y., Smeltzer, C. and Boersma, K.: Anthropogenic emissions of NOx over China:

391   Reconciling the difference of inverse modeling results using GOME-2 and OMI measurements,

392   J Geophys Res Atmospheres, 119(12), 7732–7740, doi:10.1002/2014JD021644, 2014.

393   Hoek, G., Eeftens, M., Beelen, R., Fischer, P., Brunekreef, B., Boersma, K. and Veefkind, P.:

394   Satellite NO2 data improve national land use regression models for ambient NO2 in a small

395   densely   populated   country,   Atmos   Environ,   105,   173–180,

396   doi:10.1016/j.atmosenv.2015.01.053, 2015.

397   Hudman, Russell, Valin and Cohen: Interannual variability in soil nitric oxide emissions over the

398   United States as viewed from space, Atmos Chem Phys, 10(20), 9943–9952, doi:10.5194/acp-

399   10-9943-2010, 2010.

400   Itahashi, S., Uno, I., Irie, H., Kurokawa, J.-I. and Ohara, T.: Regional modeling of tropospheric

401   NO2 vertical column density over East Asia during the period 2000–2010: comparison with

Atmospheric
Chemistry
and Physics
Discussions

402   multisatellite observations, Atmos Chem Phys, 14(7), 3623–3635, doi:10.5194/acp-14-3623-

403   2014, 2014.

404   Jaeglé, L., Steinberger, L., Martin, R. and Chance, K.: Global partitioning of NO_x sources using

405   satellite observations: Relative roles of fossil fuel combustion, biomass burning and soil

406   emissions, Faraday Discuss, 130(0), 407–423, doi:10.1039/B502128F, 2005.

407   Jiang, Z., Worden, J., Payne, V., Zhu, L., Fischer, E., Walker, T. and Jones, D.: Ozone export from

408   East Asia: The role of PAN, J Geophys Res Atmospheres, 121(11), 6555–6563,

409   doi:10.1002/2016JD024952, 2016a.

410   Jiang, Z., Miyazaki, K., Worden, J., Liu, J., Jones, D. and Henze, D.: Impacts of anthropogenic

411   and natural sources on free tropospheric ozone over the Middle East, Atmos Chem Phys,

412   16(10), 6537–6546, doi:10.5194/acp-16-6537-2016, 2016b.

413   Kharol, S. K., Martin, R. V., Philip, S., Boys, B., Lamsal, L. N., Jerrett, M., Brauer, M., Crouse,

414   D. L., McLinden, C. and Burnett, R. T.: Assessment of the magnitude and recent trends in

415   satellite-derived ground-level nitrogen dioxide over North America, Atmos Environ, 118, 236–

416   245, doi:10.1016/j.atmosenv.2015.08.011, 2015.

417   Krotkov, N. A. and Veefkind, P.: OMI/Aura Nitrogen Dioxide (NO_2) Total and Tropospheric

418   Column 1-orbit L2 Swath 13x24 km V003, Greenbelt, MD, USA, Goddard Earth Sciences

419   Data and Information Services Center (GES DISC), 2006.

420   Krotkov, N., McLinden, C., Li, C., Lamsal, L., Celarier, E., Marchenko, S., Swartz, W., Bucsela,

421   E., Joiner, J., Duncan, B., Boersma, K., Veefkind, J., Levelt, P., Fioletov, V., Dickerson, R.,

422   He, H., Lu, Z. and Streets, D.: Aura OMI observations of regional SO_2 and NO_2 pollution

423   changes from 2005 to 2015, Atmos Chem Phys, 16(7), 4605–4629, doi:10.5194/acp-16-4605-

424   2016, 2016.

Atmospheric
Chemistry
and Physics
Discussions

425   Lamsal, L., Martin, R., Padmanabhan, A., Donkelaar, A., Zhang, Q., Sioris, C., Chance, K., Kurosu,

426   T. and Newchurch, M.: Application of satellite observations for timely updates to global

427   anthropogenic NOx emission inventories, Geophys Res Lett, 38, L05810,

428   doi:10.1029/2010GL046476, 2011.

429   Lamsal, L., Duncan, B., Yoshida, Y., Krotkov, N., Pickering, K., Streets, D. and Lu, Z.: U.S. NO2

430   trends (2005–2013): EPA Air Quality System (AQS) data versus improved observations from

431   the Ozone Monitoring Instrument (OMI), Atmos Environ, 110, 130–143,

432   doi:10.1016/j.atmosenv.2015.03.055, 2015.

433   Liang, Q., Jaeglé, L., Jaffe, D., Weiss-Penzias, P., Heckman, A. and Snow, J.: Long-range transport

434   of Asian pollution to the northeast Pacific: Seasonal variations and transport pathways of

435   carbon monoxide, J Geophys Res Atmospheres 109, D23S07, doi:10.1029/2003JD004402,

436   2004.

437   Lin, M., Horowitz, L., Oltmans, S., Fiore, A. and Fan, S.: Tropospheric ozone trends at Mauna

438   Loa Observatory tied to decadal climate variability, Nat Geosci, 7(2), 136–143,

439   doi:10.1038/ngeo2066, 2014.

440   Liu, F., Zhang, Q., A, R., Zheng, B., Tong, D., Yan, L., Zheng, Y. and He, K.: Recent reduction

441   in NO x emissions over China: synthesis of satellite observations and emission inventories,

442   Environ Res Lett, 11(11), 114002, doi:10.1088/1748-9326/11/11/114002, 2016.

443   Logan, J., Staehelin, J., Megretskaia, I., Cammas, J. -P., Thouret, V., Claude, H., Backer, H.,

444   Steinbacher, M., Scheel, H. -E., Stübi, R., Fröhlich, M. and Derwent, R.: Changes in ozone

445   over Europe: Analysis of ozone measurements from sondes, regular aircraft (MOZAIC) and

446   alpine surface sites, J Geophys Res Atmospheres 117, D09301, doi:10.1029/2011JD016952,

447   2012.

448   Martin, R., Jacob, D., Chance, K., Kurosu, T., Palmer, P. and Evans, M.: Global inventory of

449   nitrogen oxide emissions constrained by space-based observations of NO2 columns, J Geophys

450   Res Atmospheres 108(D17), 4537, doi:10.1029/2003JD003453, 2003.

451   Mijling, B. and A, R.: Using daily satellite observations to estimate emissions of short-lived air

452   pollutants on a mesoscopic scale, J Geophys Res Atmospheres 117, D17302,

453   doi:10.1029/2012JD017817, 2012.

454   Miyazaki, K., Eskes, H., Sudo, K., Boersma, K., Bowman, K. and Kanaya, Y.: Decadal changes

455   in global surface NOx emissions from multi-constituent satellite data assimilation, Atmos

456   Chem Phys, 17(2), 807–837, doi:10.5194/acp-17-807-2017, 2017.

457   Parrish, D., Law, K., Staehelin, J., Derwent, R., Cooper, O., Tanimoto, H., Volz-Thomas, A., Gilge,

458   S., Scheel, H.-E., Steinbacher, M. and Chan, E.: Long-term changes in lower tropospheric

459   baseline ozone concentrations at northern mid-latitudes, Atmos Chem Phys, 12(23), 11485–

460   11504, doi:10.5194/acp-12-11485-2012, 2012.

461   Parrish, D., Lamarque, J. -F., Naik, V., Horowitz, L., Shindell, D., Staehelin, J., Derwent, R.,

462   Cooper, O., Tanimoto, H., Volz-Thomas, A., Gilge, S., Scheel, H. -E., Steinbacher, M. and

463   Fröhlich, M.: Long-term changes in lower tropospheric baseline ozone concentrations:

464   Comparing chemistry-climate models and observations at northern midlatitudes, J Geophys

465   Res Atmospheres, 119(9), 5719–5736, doi:10.1002/2013JD021435, 2014.

466   Reuter, Buchwitz, Hilboll, Richter, Schneising, Hilker, Heymann, Bovensmann and Burrows:

467   Decreasing emissions of NOx relative to CO2 in East Asia inferred from satellite observations,

468   Nat Geosci, 7(11), 792–795, doi:10.1038/ngeo2257, 2014.

469   Russell, A., Valin, L. and Cohen, R.: Trends in OMI NO2 observations over the United States:

470   effects of emission control technology and the economic recession, Atmos Chem Phys, 12(24),

Atmospheric
Chemistry
and Physics
Discussions

471   12197–12209, doi:10.5194/acp-12-12197-2012, 2012.

472   Schumann U, Huntrieser H (2007) The global lightning-induced nitrogen oxides source.

473   Atmos Chem Phys 7(14):3823{3907, doi:10.5194/acp-7-3823-2007.

474   Skowron, A., Lee, D. and León, R.: Variation of radiative forcings and global warming potentials

475   from   regional   aviation   NOx   emissions,   Atmos   Environ,   104,   69–78,

476   doi:10.1016/j.atmosenv.2014.12.043, 2015.

477   Tong, D., Lamsal, L., Pan, L., Ding, C., Kim, H., Lee, P., Chai, T., Pickering, K. and Stajner, I.:

478   Long-term NOx trends over large cities in the United States during the great recession:

479   Comparison of satellite retrievals, ground observations, and emission inventories., Atmos

480   Environ 107, 70–84, 2015.

481   Trenberth, K. E.: The Definition of El Niño, Bulletin of the American Meteorological Society,

482   *78*(12), 2771-2777, 1997.

483   van der A, R. J., Mijling, B., Ding, J., Koukouli, M. E., Liu, F., Li, Q., Mao, H., and Theys, N.:

484   Cleaning up the air: effectiveness of air quality policy for SO_2 and NO_x emissions in China,

485   Atmos. Chem. Phys., 17, 1775-1789, doi:10.5194/acp-17-1775-2017, 2017.

486   Verstraeten, W., Neu, J., Williams, J., Bowman, K., Worden, J. and Boersma, K.: Rapid increases

487   in tropospheric ozone production and export from China, Nat Geosci, 8(9), 690–695,

488   doi:10.1038/ngeo2493, 2015.

489   Ye, C., Zhou, X., Pu, D., Stutz, J., Festa, J., Spolaor, M., Tsai, C., Cantrell, C., Mauldin, R.,

490   Campos, T., Weinheimer, A., Hornbrook, R., Apel, E., Guenther, A., Kaser, L., Yuan, B., Karl,

491   T., Haggerty, J., Hall, S., Ullmann, K., Smith, J., Ortega, J. and Knote, C.: Rapid cycling of

492   reactive nitrogen in the marine boundary layer, Nature, 532(7600), 489–491,

493   doi:10.1038/nature17195, 2016.

494

495   **Tables and Figures**

496   **Figure 1.** (a-b): monthly mean (dash lines) and annual mean (solid lines) tropospheric NO_2 column
497   over contiguous United States and East China from OMI (NASA and DOMINO) products; (c-e):
498   percent changes of annual mean (c) and seasonal mean (d-e) tropospheric NO_2 column over the
499   US from the OMI and EPA's emission estimates, normalized at 2009.

501   **Figure 2.** Schematic figure showing the sources of tropospheric NO_x.

503   **Figure 3.** (a) difference of mean NO_2 concentrations of surface in-situ measurements (AQS and
504   NAPS stations) from 2009-2010 to 2014-2015; Blue (red) means decrease (increase) of NO_2
505   concentrations. (b) same as panel a, but averaged with 4°x5° resolution.

507   **Figure 4.** Flash rate density ($1x10^{-3}$ flash/km^2/month) over North America (15°N-42.5°N, 130°W-
508   60°W) from Lightning Imaging Sensor (LIS).

510   **Figure 5.** (a-f) annual slope of tropospheric NO_2 column (unit $1x10^{15}$ molec/cm^2) from OMI
511   (NASA and DOMINO products); (g-h) same as panels a-f, with percent (%) as unit.

513   **Figure 6.** (a-c) Annual slope of passive tracer column (percent base). The passive tracer is
514   simulated with GEOS-Chem model with constant 15-day lifetime. The surface NO_x emissions are
515   fixed at 2005 level. The lightning NO_x emissions are not included in the simulation. (d) Blue line:
516   regional mean (box in panel a) of passive tracer column, normalized by the 11-year mean (2005-
517   2015). The black line shows the NOAA Niño 3.4 index.

519   **Figure 7.** Seasonal mean passive tracer column (2005-2015), with 10^{16} molec cm^{-2}. The passive
520   tracer is simulated with GEOS-Chem model with constant 15-day lifetime. The surface NO_x
521   emissions are fixed at 2005 level. It should be noticed that the actual transpacific transport of
522   reactive nitrogen in fall and winter is stronger than panels c-d due to the decrease of temperature.

523
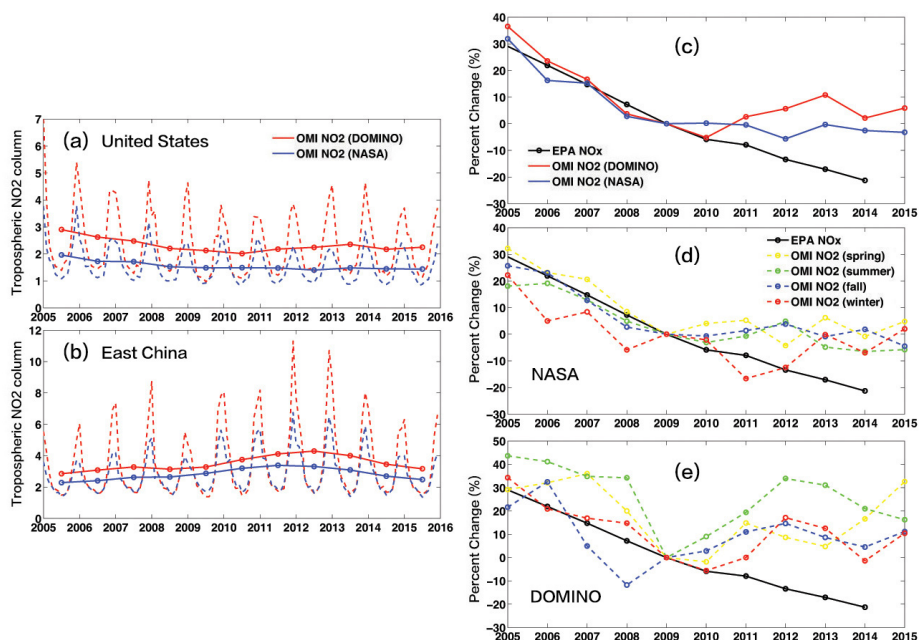
Figure 1. (a-b): monthly mean (dash lines) and annual mean (solid lines) tropospheric NO_2
column over contiguous United States and East China from OMI (NASA and DOMINO)
products; (c-e): percent changes of annual mean (c) and seasonal mean (d-e) tropospheric NO_2
column over the US from the OMI and EPA's emission estimates, normalized at 2009.

528

529
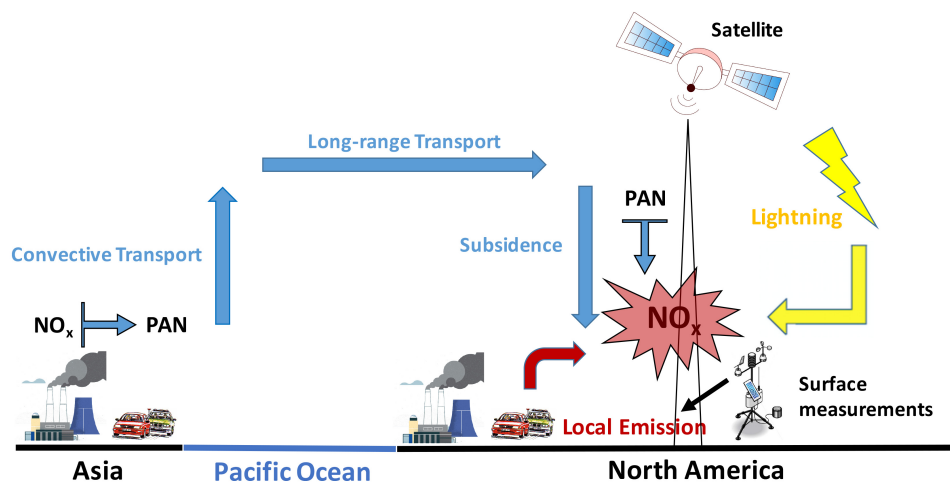
Figure 2. Schematic figure showing the sources of tropospheric NO_x.

531

532

533
534
535
536
537
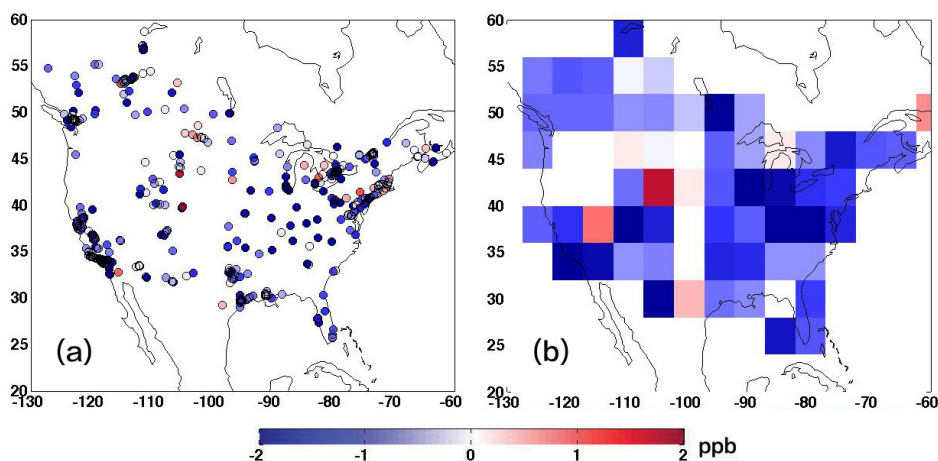
538
Figure 3. (a) difference of mean NO$_2$ concentrations of surface in-situ measurements (AQS
and NAPS stations) from 2009-2010 to 2014-2015; Blue (red) means decrease (increase) of
NO$_2$ concentrations. (b) same as panel a, but averaged with 4°x5° resolution.
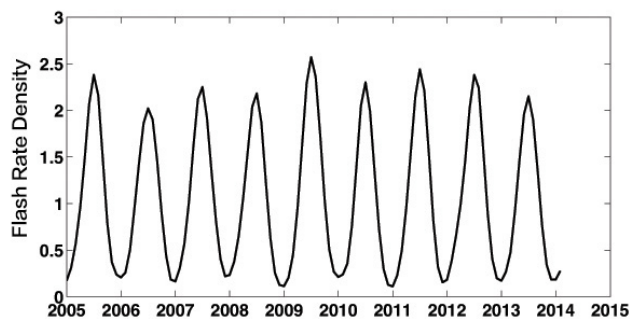
542
543
544
545
546

547
Figure 4. Flash rate density (1x10^{-3} flash/km^2/month) over North America (15°N-42.5°N,
130°W-60°W) from Lightning Imaging Sensor (LIS).

550
551
552
553
554

555

556

557

558

559

560

561

562

563

Figure 5. (a-f) annual slope of tropospheric NO$_2$ column (unit 1×10^{15} molec/cm^2) from OMI (NASA and DOMINO products); (g-h) same as panels a-f, with percent (%) as unit.
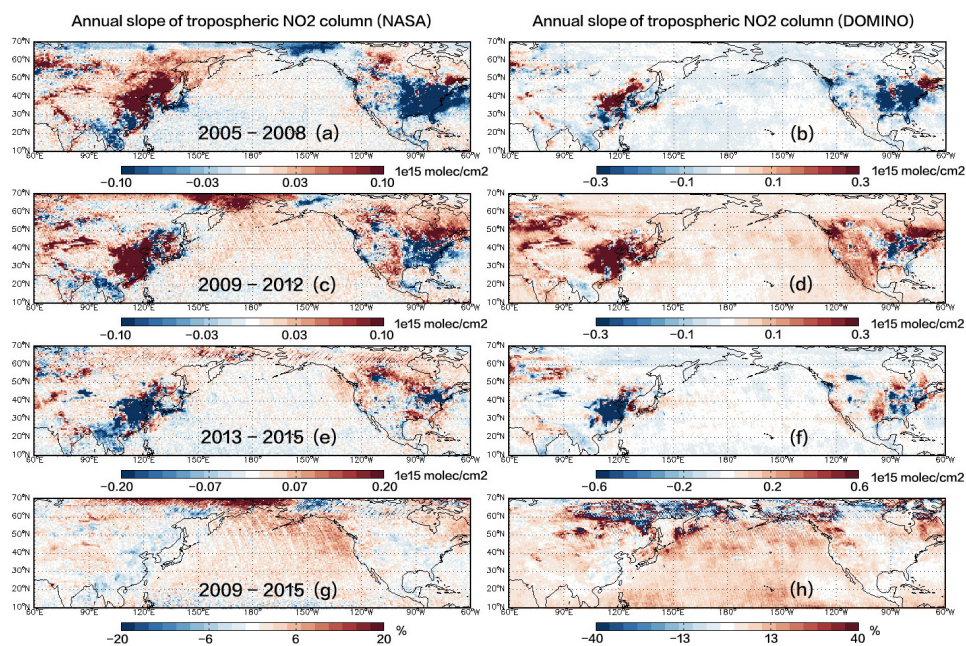
566

567

568

569

570

571

572

573

574

575

576

577

578

579

580
581
582
583
584
585
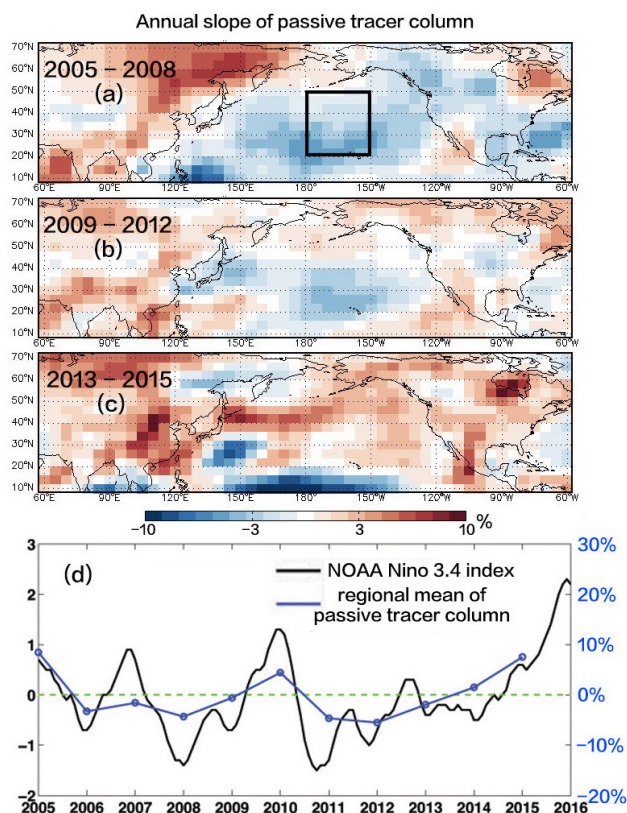
586
Figure 6. (a-c) Annual slope of passive tracer column (percent base). The passive tracer is simulated with GEOS-Chem model with constant 15-day lifetime. The surface NO_x emissions are fixed at 2005 level. The lightning NO_x emissions are not included in the simulation. (d) Blue line: regional mean (box in panel a) of passive tracer column, normalized by the 11-year mean (2005-2015). The black line shows the NOAA Niño 3.4 index.
592

Figure 7. Seasonal mean passive tracer column (2005-2015), with 10^{16} molec cm^{-2}. The passive tracer is simulated with GEOS-Chem model with constant 15-day lifetime. The surface NO$_x$ emissions are fixed at 2005 level. It should be noticed that the actual transpacific transport of reactive nitrogen in fall and winter is stronger than panels c-d due to the decrease of temperature.